LDA+U Study on Fully Relaxed LaTiO$_3$ and (SrTiO$_3$)$_m$(LaTiO$_3$)$_n$ Superlattice Structures

Hyo-Shin AHN

Future Technology Research Division, Korea Institute of Science and Technology, Seoul 136-791 and
Center for Strongly Correlated Materials Research, Seoul National University, Seoul 151-742

Do Duc CUONG and Jaichan LEE

Department of Materials Science, Sungkyunkwan University, Suwon 440-746

Seungwu HAN*

Department of Physics, Ewha Womans University, Seoul 120-750

Using LDA+U (where LDA stands for local-density-approximation and U for on-site coulomb energy) method, we study the structural and electronic properties of LaTiO$_3$ and (SrTiO$_3$)$_m$(LaTiO$_3$)$_n$ superlattice structures. Lattice vectors, as well as ionic positions, are relaxed to minimize the LDA+U energy functional. We find that the inclusion of the U term increases the lattice parameters and leads to larger distortions of oxygen octahedra in LaTiO$_3$ and that the overall agreement with experiment is improved compared to LDA results. In the superlattice, we find that octahedral distortions around the La layer lower the total energy. The ionic relaxations, especially those of Ti atoms near the La layer, affect the spatial distribution of doped electrons, leading to a broader charge profile than the case without ionic relaxation. The corresponding Ti^{3+} profile is in good agreement with the electron-energy-loss spectroscopy data.

I. INTRODUCTION

The ABO$_3$-type perovskite transition-metal oxides cover a wide range of material properties. Depending on the valence states and the sizes of cations at the A or the B sites, material properties change drastically from insulating to metallic, from non-magnetic to magnetic, and from paraelectric to ferroelectric. Behind this variety of physical properties are the intricate exchange-correlation interactions between d electrons at B sites which are mediated by oxygen p orbitals. Many theoretical and experimental efforts have been brought to elucidate the relation between various compositional parameters and the structural and the electronic properties of perovskite oxides.

The density functional theory [1] has been successful in investigating many different kinds of materials. However, the application of the method to transition-metal oxides has been particularly limited in many cases. This is largely due to the strong electron-electron correlations between localized d electrons, where is beyond the scope of the conventional local density approximation (LDA) or the generalized gradient approximation (GGA). In the case of Mott insulators such as NiO, LaTiO$_3$, and YTiO$_3$, however, correlation effects are based on the relatively simple physics of the on-site Hubbard U energy, which is defined as the Coulomb energy experienced by an extra d electron occupying the Ni or the Ti sites. Several methods at different levels of approximation have been applied to solve the constructed Hubbard Hamiltonians. For example, the dynamic mean-field theory [2], Hartree-Fock approximation [3], and LDA+U [4] method have been exploited. Among them, the LDA+U formalism treats the on-site Coulomb interaction through orbital-dependent potentials that involve empirical parameters related to on-site (U) and exchange (J) interactions. This method requires moderate computational resources comparable to conventional density functional calculations. In addition, the functional is variational, allowing for geometry optimization. The application of LDA+U methods to several transition metal oxides has shown satisfactory results for the energy gap and magnetic ordering [4].

SrTiO$_3$ and LaTiO$_3$ are electronic insulators with energy gaps of 3.2 and 0.1 $\sim$ 0.2 eV, respectively. However,

*E-mail: hansw@ewha.ac.kr; Fax: +82-2-3277-2372

the origin of the insulating behavior is fundamentally different. SrTiO$_3$ is a charge-transfer insulator where the energy gap is related to the excitation of O-2p orbitals to Ti-3d orbitals. On the other hand, LaTiO$_3$ is a well-known Mott insulator, and on-site Coulombic interactions play a key role in determining the energy gap. As mentioned above, the insulating property of LaTiO$_3$ is not properly described by the conventional LDA or GGA methods because these methods predict LaTiO$_3$ to be metallic. Instead, the LDA+U scheme taking into account the localized nature of Ti-3d orbital was shown to reproduce the insulating behavior with the correct magnetic ordering [5]. Recently, the LDA+U method was applied to superlattices consisting of SrTiO$_3$ and LaTiO$_3$ [6]. The localized charges transferred from the La layer necessitate a proper description of d-orbital occupation.

While the LDA+U calculation has become increasingly popular for studying the transition-metal oxides, little information is available on relaxed structures and the accompanying changes in electronic structure consistent with the employed computational method. Most of LDA+U studies on the ABO_3 perovskite compounds were carried out with ionic positions and structural parameters given by experimental data [2, 5]. It is well documented that the material properties of perovskite oxides are sensitive to the external strain. For example, magneto-transport property change in strained LaAlO$_3$ [Ref. 1], room-temperature ferroelectricity [7], and latltce instability [Ref. 2] in strained SrTiO$_3$ were observed [8]. Therefore, in this work, we investigate the electronic and the structural properties of fully relaxed LaTiO$_3$ and (SrTiO$_3$)$_m$(LaTiO$_3$)$_n$ superlattices by using LDA+U methods with an aim to establish self-consistent predictions for these materials.

This paper is organized as follows: In Section II, we introduce the computational methods employed in this work. We apply LDA+U methods to LaTiO$_3$ with two sets of U and J parameters in Section III.1 and extend the application to (SrTiO$_3$)$_m$(LaTiO$_3$)$_n$ in Section III.2 We summarize and conclude in Section IV.

II. THEORY

Throughout this work, we use the Vienna $Ab-initio$ Simulation Package (VASP) for the first-principles calculations [10]. The projector-augmented wave (PAW) pseudopotentials [11] are employed to describe the electron-ion interaction. The valence configurations are $[4s^24p^6]5s^2$, $[5s^25p^6]6s^25d^14f^0$, $[3s^23p^6]4s^23d^2$, and $2s^22p^4$ for Sr, La, Ti, and O atoms, respectively. (The semicore states are bracketed.) The atomic positions are relaxed until the Hellmann-Feynman force on each atom is reduced to within 0.05 eV/Å. The energy cutoff is chosen to be 500 eV. The 6 × 6 × 6 and 4 × 4 × 2 Monkhorst-Pack grids are employed in the Brillouin zone integration for SrTiO$_3$ and LaTiO$_3$, respectively.
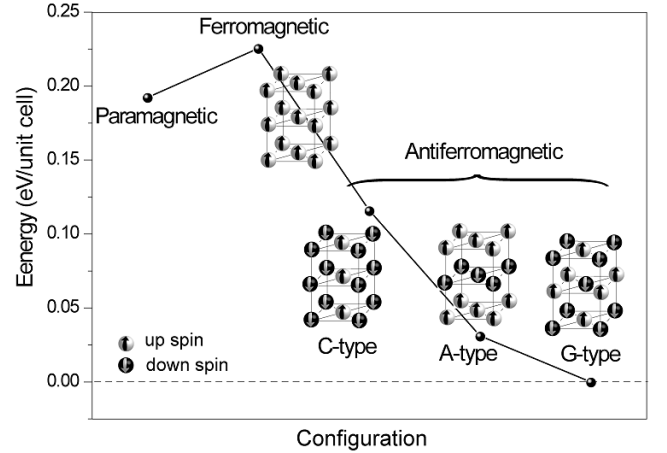

Fig. 1. Total energies of fully relaxed LaTiO$_3$ with various magnetic orderings of d electrons at Ti sites. The energy zero is set to the total energy of the antiferromagnetic G-type ordering, which is most stable.

For plotting the density of states, we sampled k-points on denser meshes. This combination of energy cutoff and k-point sampling ensures the convergence of total energies to within 5 meV/atom. The Fermi-Dirac broadening is used with a width of 0.02 eV. The equilibrium lattice parameters of the crystalline phase are obtained by minimizing the magnitudes of stress tensors under 0.5 kbar.

We follow the LDA+U formalism as implemented into VASP. We the reader refer to Ref. 10 for a detailed overview. We have used two sets of values, (3.2, 0.9) eV and (5, 0.64) eV, for the (U, J) parameters describing the on-site screened Coulomb energy and exchange interactions. The first set is obtained from the constrained density functional calculations assuming partial localization of d-states whereas the second one reflects a picture in where all d electrons are localized [5]. In LaTiO$_3$, where the e_g levels are unoccupied, the first choice for U and J looks more reasonable. As we will show below, this is confirmed in the density of states compared with extant experimental data. We employ the spherically symmetric approach to the LDA+U functional, as proposed in Ref. 11, where the model Hamiltonian describing the on-site interaction depends only on U-J.

III. RESULTS

1. LaTiO$_3$

We first look into the structural properties of fully relaxed LaTiO$_3$. Several LDA+U approaches have been applied to this material [2,5,14]. LaTiO$_3$ is a GdFeO$_3$-type orthorhombic structure, and the unit cell, where is characterized by three lattice parameters (a, b, and c), contains four transition-metal ions. At low temperatures, LaTiO$_3$ is G-type antiferromagnetic with $T_N =$

Table 1. The lattice parameters, orthorhombic distortion ($\epsilon = (b-a)/(b+a)$), internal coordinates, magnetic moment (m), and optical and charge-transfer energy gaps of the fully relaxed LaTiO$_3$ are compared with experiment and other theoretical results. O1 and O$_2$ indicate the apical and basal O atoms. The internal positions of the atoms in the unit cell are as follows: La: (x_{La}, y_{La}, 1/4), (1/2$-x_{La}$, 1/2$+y_{La}$, 1/4), ($-x_{La}$, $-y_{La}$, 3/4),(1/2$+x_{La}$, 1/2$-y_{La}$, 3/4) / Ti: (0, 1/2, 0), (1/2, 0, 0), (0, 1/2, 1/2), (1/2, 0, 1/2) / O1: (x_{O1}, y_{O1}, 1/4), (1/2$-x_{O1}$, 1/2$+y_{O1}$, 1/4), ($-x_{O1}$, $-y_{O1}$, 3/4),(1/2$+x_{O1}$, 1/2$-y_{O1}$, 3/4) / O2: (x_{O2}, y_{O2}, z_{O2}), (x_{O2}, y_{O2}, 1/2$-z_{O2}$), ($-x_{O2}$, $-y_{O2}$, $-z_{O2}$), ($-x_{O2}$, $-y_{O2}$, 1/2$+z_{O2}$), (1/2$-x_{O2}$, 1/2$+y_{O2}$, z_{O2}), (1/2$-x+O2$, 1/2$+y_{O2}$, 1/2$-z_{O2}$), (1/2$+x_{O2}$, 1/2$-y_{O2}$, $-z_{O2}$), (1/2$+x_{O2}$, 1/2$-y_{O2}$, 1/2$+z_{O2}$).

	Exp.[1]	Theory[2]	LDA $U = J = 0$	$U = 3.2$ eV $J = 0.9$ eV	$U = 5$ eV $J = 0.64$ eV
a(Å)	5.644	5.602	5.462	5.586	5.602
b(Å)	5.589	5.712	5.524	5.529	5.712
c(Å)	7.901	7.899	7.799	7.789	7.899
	-0.0049	0.0097	0.0056	-0.0051	0.0097
x_{La}	0.99303	0.98626	0.99478	0.99268	0.98659
y_{La}	0.04912	0.04399	0.04126	0.05697	0.06077
z_{La}	0.25	0.25	0.25	0.25	0.25
x_{O1}	0.09133	0.07262	0.06205	0.08069	0.09358
y_{O1}	0.49403	0.48587	0.49026	0.49711	0.48442
z_{O1}	0.25	0.25	0.25	0.25	0.25
x_{O2}	0.70923	0.71763	0.70947	0.70642	0.70490
y_{O2}	0.29433	0.28028	0.28902	0.29690	0.29817
z_{O2}	0.04281	0.03882	0.03236	0.04204	0.04907
$m(\mu_B)$	0.45	-	0	0.58	0.8
E_g^{op}(eV)	0.1 $\sim$ 0.2[3]	-	0	0.16	1.5
E_g^{CT}(eV)	4.5[4]	-	-	3.6	3.97

[1] Ref. 13 [2] Ref. 14; GGA functional was used. [3] Ref. 15, 16 [4] Ref. 16.

150 K [15]. In Fig. 1, we compare the relative energetics for various magnetically ordered structures. The parameters used for LDA+U are $U = 3.2$ eV and $J = 0.9$ eV. Both the lattice parameters and the internal positions of ions are fully relaxed. G-type antiferromagnetic ordering is found to be the most stable, in good agreement with experiment. In Table 1, the computed lattice parameters and fractional coordinate of each ion of G-type antiferromagnetic LaTiO$_3$ are displayed. One can observe that a large U parameter tends to increase the lattice parameters and enlarge the octahedral distortion. It is notable that the orthorhombic distortion defined by $\epsilon = (b-a)/(b+a)$ is correctly estimated when the LDA+U method is applied with $U = 3.2$ eV and $J = 0.9$ eV. The sign of ϵ is positive if the octahedron undergoes a rigid tilt through the b axis. The negative sign means that the basal plane formed by four oxygen atoms (O2 atoms in Table 1) is transformed from a square into a rectangle. In fact, we find that the edge of basal plane along the a axis is elongated by 3.6 % for $U = 3.2$ eV. This is in excellent agreement with experimental data reporting 4 % Jahn-Teller distortion [15]. The magnetic moment of LaTiO$_3$ is 0.58 μ_B, which is substantially smaller than previous calculations 0.8 $\sim$ 1.0 μ_B [5,14] and closer to experimental values. The reduced magnetic moment is related to the lattice parameter that is smaller

than experimental values; if calculations are performed with experimentally reported structures, the overlap integral between Ti-d and O-p orbitals is reduced, and this results in a more localized picture of Ti-d states. In the case of $U = 5$ eV, the magnetic moment is close to one Bohr magneton, indicating a full localization of Ti-d orbitals. To check the dependence on the approximated density functional, we also carry out a calculation with spin-polarized GGA+U. The overall lattice parameters systematically increase by 2 $\sim$ 3 % compared to LDA data, and the degree of distortion is increased.

In Fig. 2, the density of states (DOS) of fully relaxed LaTiO$_3$ are compared between LDA and LDA+U methods using two sets of U and J parameters. As is well established, a metallic character is found with LDA while a band gap opening is observed with LDA+U methods. In the DOS of the fully relaxed LaTiO$_3$ structure with the value of $U = 3.2$ eV and $J = 0.9$ eV, the fundamental energy gap is 0.16 eV, and the charge transfer gap is 3.6 eV. On the other hand, for a larger value of $U = 5$ eV, the gaps increase to 1.5 eV and 3.97 eV, respectively. Again, the first set of parameters is in better agreement with experiments, where observe small energy gaps of $\sim$0.05 eV (fundamental gap at 6 K) [19] and $\sim$4.5 eV (charge transfer gap) [18]. The decomposition of states into t_{2g} and e_g orbitals of the Ti atom shows the t_{2g} character of
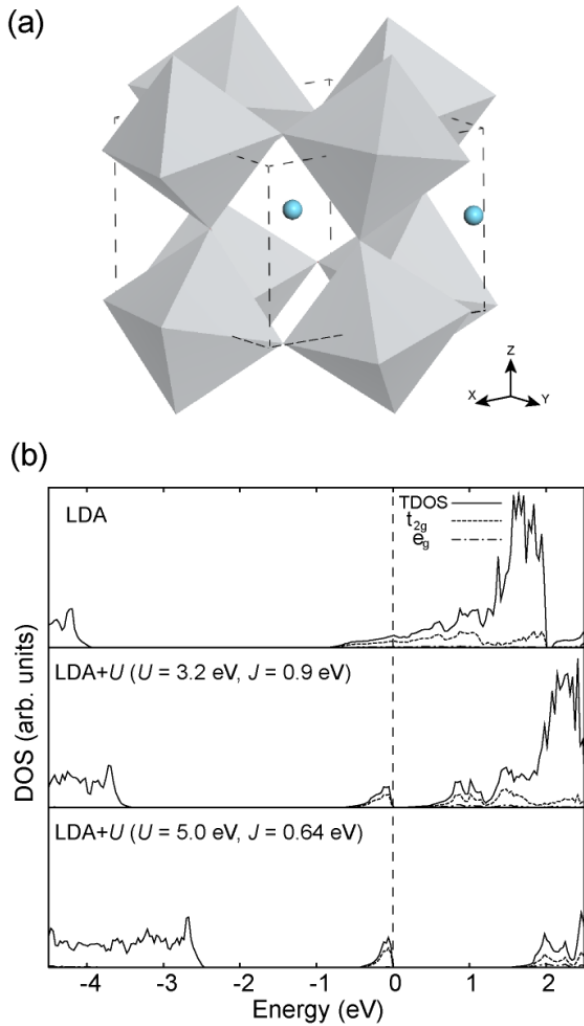
Fig. 2. (a) Unit cell of LaTiO$_3$. The six corners of each octahedron are formed by O atoms, and spheres indicate La atoms. (b) Total density of states (TDOS) and partial density of states of LaTiO$_3$. Due to the non-cubic geometry, the decomposition into t_{2g} and e_g characters is slightly intermixed. Near the Fermi level (set to zero), most Ti-d states have t_{2g} characters. For plotting the DOS, we sampled $10 \times 10 \times 8$ mesh points in the first Brillouin zone.

Fig. 3. Density of states for SrTiO$_3$ with various values of U and J. The density of states are drawn using k-points on a $14 \times 14 \times 14$ mesh to capture the valence maximum and the conduction minimum precisely. The shapes of the valence and the conduction bands are maintained with only a shift in the relative position.

conduction states.

In passing, we apply the LDA+U method to SrTiO$_3$. Since the Ti-d orbital is almost empty in crystalline SrTiO$_3$, the effect of the LDA+U method should be minimal. The equilibrium lattice parameter found with LDA is 3.866 Å, compared to the experimental value of 3.905 Å. Applying the LDA+U calculation with $U = 3.2$ eV and $J = 0.9$ eV increases the lattice parameter to 3.881 Å, a lattice expansion similar to the case of LaTiO$_3$. On the other hand, the indirect band gap ($\Gamma \to M$) is found to be 2.21 eV. This is a large increase from the LDA value of 1.92 eV and compares favorably with the experimental measurement of 3.2 eV. A further increase in the U value up to 5 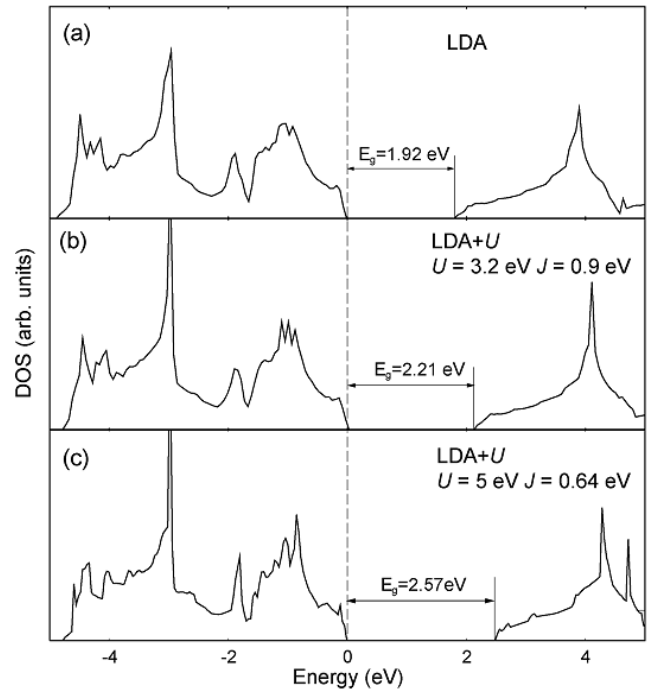eV enlarges the energy gap to 2.57 eV. In Fig. 3, the densities of states for SrTiO$_3$ with the LDA and the LDA+U methods are presented. The shapes of the valence and the conduction bands are almost unchanged, except for the energy gap between them.

2. (SrTiO$_3$)$_m$(LaTiO$_3$)$_1$ Superlattice

Next, we calculate the (SrTiO$_3$)$_m$(LaTiO$_3$)$_1$ superlattice structures, which can be conceived of as bulk SrTiO$_3$ with planar LaTiO$_3$ layers periodically embedded. The difference in the valence states of La and Sr atoms (3+ versus 2+) results in a free electronic carrier per each La site, and its spatial distribution has been of particular interest experimentally, as well as theoretically [6, 20,21]. Our model superlattice develops along the z-axis with in-plane lattice parameters constrained to those of SrTiO$_3$. This reflects the underlying thick SrTiO$_3$ substrate used in the experiment. In Ref. 19, various kinds of (SrTiO$_3$)$_m$(LaTiO$_3$)$_n$ superlattices were fabricated using a pulsed laser deposition method. The modulation of electronic charges from La was closely examined using electron-energy-loss spectroscopy, and the free electrons identified through Ti^{3+} signals were found to be localized within about three SrTiO$_3$ layers from the La layer. A recent first-principles study on the superlattice [6] showed
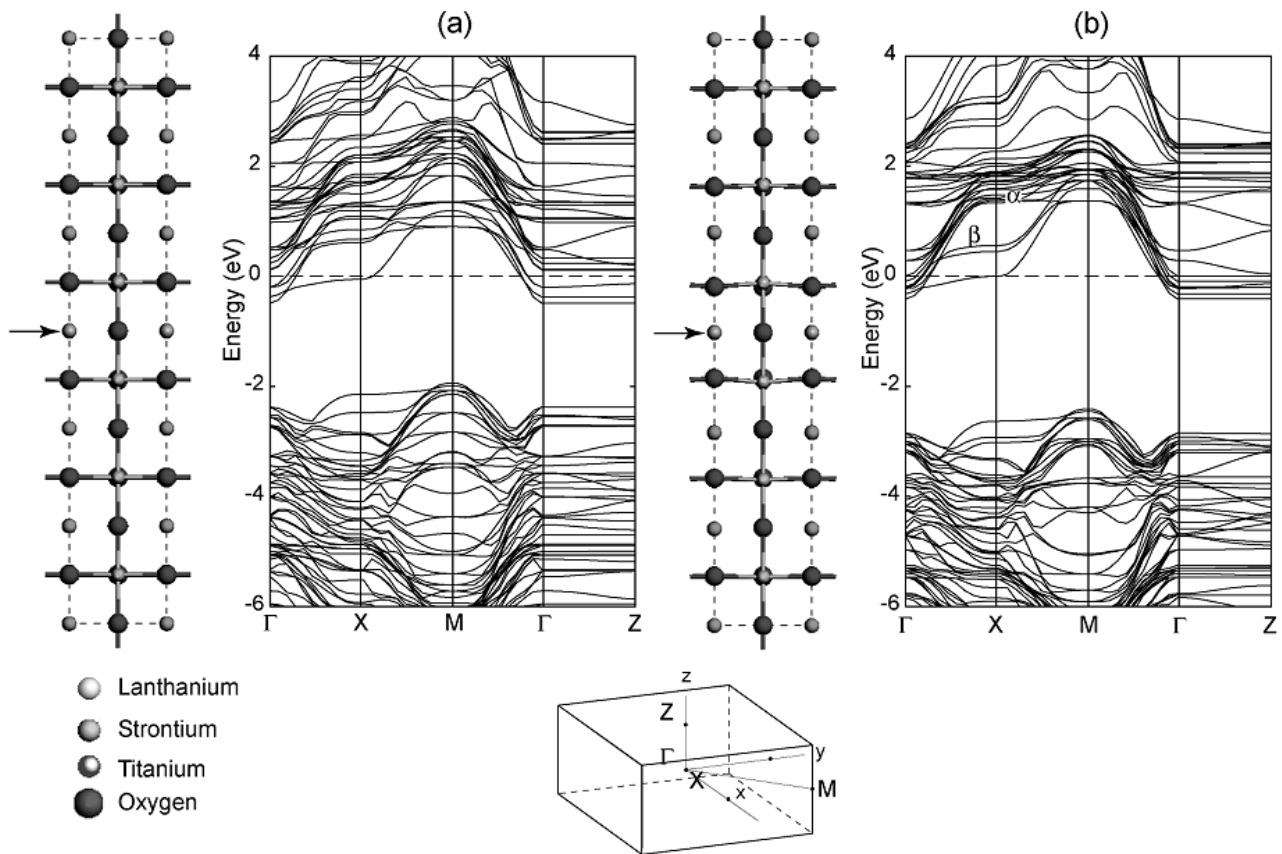
Fig. 4. Geometries and electronic structures of (a) fixed and (b) relaxed superlattices. It is noticeable that the Ti atoms near the La layer (indicated by arrows) are pushed away while the O atoms are pulled in α and β in (b) indicate up-shifted and down-shifted bands as a result of relaxation, respectively.

that the electron is mostly localized within the one TiO_2 layer closest to the La layer, which is much sharper than experimental observations. Even though not mentioned explicitly, it is likely that structural relaxation is likely missing in that work, and examining the relaxation pattern of $(SrTiO_3)_m(LaTiO_3)_n$ superlattices and its effects on the electronic structures would be worthwhile.

Firstly, the magnetic ordering in the $(SrTiO_3)_6$ $(LaTiO_3)_1$ superlattice is studied. We use $U = 3.2$ eV and $J = 0.9$ eV, which gives better results for $LaTiO_3$. The magnetic moments are found to be negligibly small, regardless of the various starting magnetization patterns. This is due to the fact that electrons transferred from La layers are rather dispersed in the spatial distribution and that d-orbital occupancies of Ti atoms are much less than one. In Fig. 4, the atomic positions and the band structures are shown with the ionic positions fixed at bulk positions (Fig. 4(a)) or fully relaxed (Fig. 4(b)) within the 1×1 lateral (xy-direction) periodicity. The Ti atoms right above and below the La layer are found to relax outward from the layer by 0.1 Å while O atoms move closer to the layer by 0.2 Å. This relaxation pattern of Ti and O atoms closely resembles the ferroelectric optical mode of $SrTiO_3$. This is because the net electro-

static charge in the $La^{3+}O^{2-}$ layer is positive. After relaxation, changes in the band structure are noticeable above the Fermi level, as indicated by α and β in Fig. 4(b). We find that those bands showing a downshift (indicated with β) are related to the Ti-d orbitals while the up-shifted bands (shown as α) are mainly composed of the f orbitals of La atoms.

Since octahedral distortion is observed only for $LaTiO_3$ and not for $SrTiO_3$, it is an intriguing question whether a distorted structure is more stable in superlattices. To this end, we expand the lateral periodicity to be $\sqrt{2} \times \sqrt{2}$, where can accommodate octahedral distortions similar to that of $LaTiO_3$. After ionic relaxations, we find that a structure with octahedral distortions occurring in layers closest to the La layer is more stable than a cubic 1×1 superlattice by 0.3 eV per unit cell. The degrees of titling and rotation are smaller than those of $LaTiO_3$. However, the octahedral distortion does not change the electronic structures significantly (see below). A transmission-electron-microscopy image taken at low temperatures may confirm this finding.

In Figs. 5(a) $\sim$ (c), we present the partial density of states (PDOS) for each TiO_2 layer. Before relaxation, the PDOS projected onto the first TiO_2 layer next to
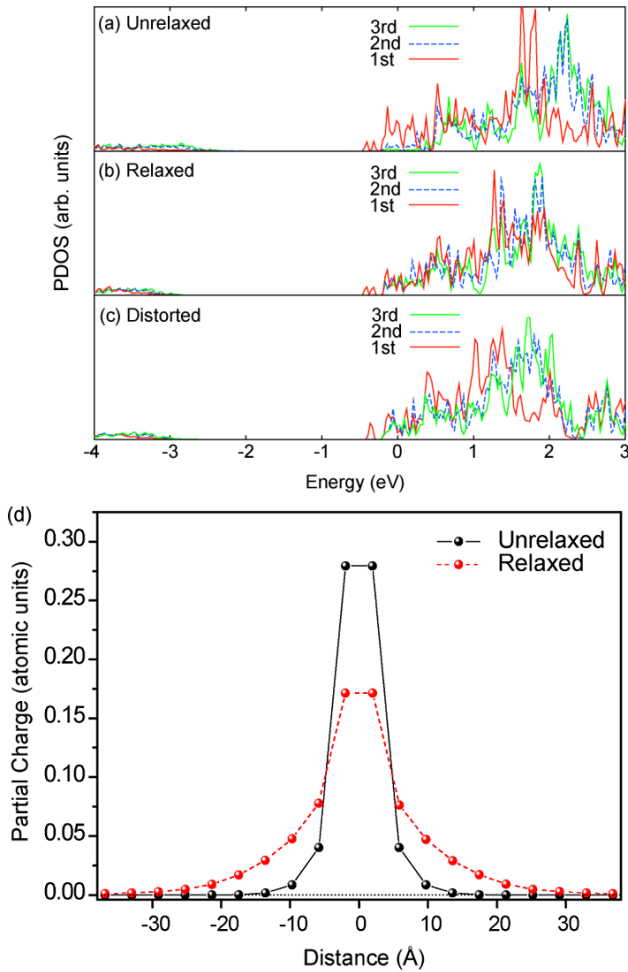
Fig. 5. (Color online) (a) $\sim$ (c) Partial density of states of $(SrTiO_3)_5(LaTiO_3)_1$ projected onto each Ti atom ordered from the La layer. (the 1*st* layer is closest to the La layer.) The Fermi level is set to zero. (d) The distribution of partial charges at Ti sites is shown for electrons in the conduction band. This corresponds to the profile of the chemical state Ti^{3+}. A longer period superlattice is used for $(SrTiO_3)_{19}(LaTiO_3)_1$ to examine the decaying tails. The origin corresponds to the position of the La layer.

the La layer is pronounced near the Fermi level. On the other hand, in the relaxed configuration, the charge distribution becomes much broader. The positive charge in the La layer is substantially screened by the dipole moments associated with a ferroelectric mode, and all Ti atoms are under the similar influence of the charged layer. On the other hand, the octahedral distortion does not affect the PDOS noticeably near the Fermi level as shown in Fig. 5(c).

In order to investigate the chemical states of Ti atoms for comparison with the experimental electron-energy-loss-spectroscopy (EELS) data [21], we calculate the partial charges by projecting electrons in the conduction band onto Ti atoms and we plot the results in Fig. 5(d). To obtain a fully decaying behavior of

the charge distribution, we use a longer supercell of $(SrTiO_3)_{19}(LaTiO_3)_1$. The distribution with atoms fixed at bulk positions shows a sharp profile close to the La layer. This is similar to the one reported in Ref. 6. After relaxation, the distribution is broadened and the electrons spill to neighboring Ti atoms down to several layers. This is consistent with the change in the PDOS shown in Fig. 5(a) $\sim$ (c) induced by structural relaxations. In the experiment, the EELS spectrum indicates that the Ti^{3+} profile has a full-width at half-maximum of around 5 layers. Therefore, the charge density distribution obtained with the structural relaxation is in much better agreement with experiment than that obtained without structural relaxation.

IV. SUMMARY

In this work, we have studied in detail the structural and the electronic properties of LaTiO$_3$ and $(SrTiO_3)_m(LaTiO_3)_1$ superlattices by using the LDA+U method. We found that the structural relaxation which has rarely been considered so far, gave results in better agreement with experiment. In the case of LaTiO$_3$, the sign of the orthorhombic distortion and the magnetic moment were in good agreement with the experimental measurements. In the superlattice, optical mode relaxation was found to affect the electronic profile and to produce results that were more consistent with the EELS spectrum. Our results underscore the importance of the structural relaxation in studying the oxide perovskites with the LDA+U method.

REFERENCES

[1] W. Kohn and L. J. Sham, Phys. Rev. **140**, A1133 (1965).
[2] E. Pavarini, S. Biermann, A. Poteryaev, A. I. Lichtenstein, A. Georges and O. K. Andersen, Phys. Rev. Lett. **92**, 176403 (2004).
[3] T. Mizokawa and A. Fujimori, Phys. Rev. B **54**, 5368 (1996).
[4] V. I. Anisimov, J. Zaanen and O. K. Andersen, Phys. Rev. B **44**, 943 (1991).

[5] I. Solovyev, N. Hamada and K. Terakura, Phys. Rev. B **53**, 7158 (1996).

[6] Z. S. Popovic and S. Satpathy, Phys. Rev. Lett. **94**, 176805 (2005).

[7] S. Y. Park, Y. P. Lee and V. G. Prokhorov, J. Korean Phys. Soc. **45**, 47 (2004).

[8] J. H. Haeni, P. Irvin, W. Chang, R. Uecker, P. Reiche, Y. L. Li, S. Choudhury, W. Tian, M. E. Hawley, B. Craigo, A. K. Tagantsev, X. Q. Pan, S. K. Streiffer, L. Q. Chen, S. W. Kirchoefer, J. Levy and D. G. Schlom, Nature **430**, 758 (2004).

[9] L. Kim, J. Kim and J. Lee, J. Korean Phys. Soc. **46**, 77 (2005).

[10] G. Kresse and J. Hafner, Phys. Rev. B **47**, R558 (1993); ibid. **49**, 14251 (1994).

[11] P. E. Blöchl, Phys. Rev. B **50**, 17953 (1994).

[12] A. Rohrbach, J. Hafner and G. Kresse, Phys. Rev. B **69**, 075413 (2004).

[13] S. L. Dudarev, G. A. Botton, S. Y. Savrasov, C. J. Humphreys and A. P. Sutton, Phys. Rev. B **57**, 1505 (1998).

[14] S. V. Streltsov, A. S. Mylnikova, A. O. Shorikov, Z. V. Pchelkina, D. I. Khomskii and V. I. Anisimov, Phys. Rev. B **71**, 245114 (2005).

[15] M. Cwik, T. Lorenz, J. Baier, R. Müller, G. André, F. Bourée, F. Lichtenberg, A. Freimuth, R. Schmitz, E. Müller-Hartmann and M. Braden, Phys. Rev. B **68**, 060401(R) (2003).

[16] C. J. Pickard, B. Winkler, R. K. Chen, M. C. Payne, M. H. Lee, J. S. Lin, J. A. White, V. Milman and D. Vanderbilt, Phys. Rev. Lett. **85**, 5122 (2000).

[17] D. A. Crandles, T. Timusk and J. E. Greedan, Phys. Rev. B **44**, 13250 (1991).

[18] T. Arima, Y. Tokura and J. B. Torrance, Phys. Rev. B **48**, 17006 (1993).

[19] P. Lunkenheimer, T. Rudolf, J. Hemberger, A. Pimenov, S. Tachos, F. Lichtenberg and A. Loidl, Phys. Rev. B **68**, 245108 (2003).

[20] S. Okamoto and A. J. Millis, Nature **428**, 630 (2004).

[21] A. Ohtomo, D. A. Muller, J. L. Grazul and H. Y. Hwang, Nature **419**, 378 (2002).